Original Article

http://www.jcpjournal.org
pISSN 2288-3649 · eISSN 2288-3657
https://doi.org/10.15430/JCP.2023.28.3.115

JCP

Organic Acids Derived from Saliva-amalgamated Betel Quid Filtrate Are Predicted as a Ten-eleven Translocation-2 Inhibitor

Devyani Bhatkar[1], Nistha Ananda[1], Kiran Bharat Lokhande[2], Kratika Khunteta[1], Priyadarshini Jain[1], Ameya Hebale[1], Sachin C. Sarode[3], Nilesh Kumar Sharma[1]

[1]Cancer and Translational Research Lab, Dr. D. Y. Patil Biotechnology & Bioinformatics Institute, Dr. D. Y. Patil Vidyapeeth, [2]Bioinformatics Research Laboratory, Dr. D. Y. Patil Biotechnology and Bioinformatics Institute, Dr. D. Y. Patil Vidyapeeth, [3]Department of Oral Pathology and Microbiology, Dr. D. Y. Patil Dental College and Hospital, Dr. D. Y. Patil Vidyapeeth, Pune, India

There is a lack of evidence regarding the use of betel quid (BQ) and its potential contribution to oral cancer. Limited attention has been directed towards investigating the involvement of BQ-derived organic acids in the modulation of metabolic-epigenomic pathways associated with oral cancer initiation and progression. We employed novel protocol for preparing saliva-amalgamated BQ filtrate (SABFI) that mimics the oral cavity environment. SABFI and saliva control were further purified by an in-house developed vertical tube gel electrophoresis tool. The purified SABFI was then subjected to liquid chromatography-high resolution mass spectrometry analysis to identify the presence of organic acids. Profiling of SABFI showed a pool of prominent organic acids such as citric acid. malic acid, fumaric acid, 2-methylcitric acid, 2-hydroxyglutarate, *cis*-aconitic acid, succinic acid, 2-hydroxyglutaric acid lactone, tartaric acid and β-ketoglutaric acid. SABFI showed anti-proliferative and early apoptosis effects in oral cancer cells. Molecular docking and molecular dynamics simulations predicted that SABFI-derived organic acids as potential inhibitors of the epigenetic demethylase enzyme, Ten-Eleven Translocation-2 (TET2). By binding to the active site of α-ketoglutarate, a known substrate of TET2, these organic acids are likely to act as competitive inhibitors. This study reports a novel approach to study SABFI-derived organic acids that could mimic the chemical composition of BQ in the oral cavity. These SABFI-derived organic acids projected as inhibitors of TET2 and could be explored for their role oral cancer.

Key Words Organic acids, Betel quid, Head and neck neoplasms, Antagonists & inhibitors, Mass spectrometry

INTRODUCTION

Oral cancer ranks as the sixth most prevalent cancer in the Asian population. The use of various tobacco-containing products and the habit of chewing betel quid (BQ) are closely associated with cancer-related mortality [1,2]. It is widely acknowledged that BQ usage contributes to the development of oral submucous fibrosis (OSMF), which can progress to oral squamous cell carcinoma (OSCC) [3-5]. BQ consists of a multitude of compounds, including alkaloids such as arecaidine, arecoline, arecolidine, guvacoline, guvacine, as well as sweeteners and flavoring agents [3-5].

While there exists substantial in vitro data on the DNA-damaging and anticancer properties of these alkaloids, limited information is available regarding their presence and availability within the oral cavity environment, where BQ-derived chemicals are expected to be released [6-12]. Furthermore, there is a dearth of appropriate methodologies that can accurately determine the nature and concentration of chemicals leached from BQ during the process of chewing.

Another concern is focused on certain chemicals (e.g., arecaidine and arecoline) derived from BQ for their carcinogenic effects. However, BQ contains several forms of chemicals, including sweeteners, flavoring agents, mouth fresheners, and other additives, and their solubility in the context of the oral cavity is not highlighted [5-10]. To understand the pro-OSMF-OSCC effects of BQ in the oral cavity, we need to characterize the comprehensive nature of chemicals and metabolites in a similar environment as observed while chewing BQ, along with the salivary environment and mechanical mastica-

Received June 20, 2023, Revised August 13, 2023, Accepted August 13, 2023
Correspondence to Nilesh Kumar Sharma, E-mail: nilesh.sharma@dpu.edu.in, https://orcid.org/0000-0002-8774-3020

tion process. As per the existing literature, most in vitro and limited in vivo assays focused on the extraction of BQ-derived alkaloids such as arecaidine, arecoline, arecolidine, guvacoline, and guvacine using organic solvents that led to the highly variable levels in the saliva of aerca nut (AN)/BQ chewers [3-12].

It is important to note that there are no organic solvents present in the oral cavity during BQ chewing, only solvents in the salivary environment. Therefore, it is crucial to know the chemicals and metabolites that can be referred to as organic acids derived from BQ in the salivary amalgamated environment. Different classes of chemicals and organic acids are known to possess different solubility. For example, alkaloids such as arecaidine, arecoline, arecolidine, guvacoline, and guvacine are sparingly soluble in polar water solvents and highly soluble in non-polar organic solvents. Therefore, several forms of organic acids derived from BQ along with arecaidine, arecoline, arecolidine, guvacoline, and guvacine need to be considered for a better understanding of molecular mechanisms that can contribute to OSMF-OSCC.

Emerging views on the link between modulations of epigenetic states by organic acids are well appreciated [13-18]. Saliva-amalgamated BQ filtrate (SABFI) could be one potential source of organic acids for those constantly and for an extended period exposed to oral squamous cells in the case of BQ users. Ten-Eleven Translocation-2 (TET2) is a DNA demethylase epigenetic enzyme among many epigenetic modifiers. TET2 is associated with the maintenance of chromatin in an inactive transcriptional state of protooncogenes by inducing DNA hypomethylation DNA state [19-22]. TET2 is considered a member of the tumor suppressor family of proteins. Conversely, due to mutation of TET2 or inhibition of TET2 by organic acids, cancer cells are known to achieve a DNA hypermethylation state and, in turn, transcriptional activation of oncogenes. Hence, it is necessary to understand the effects of organic acids upon TET2 and associated epigenetic alterations that may help cancer cells to acquire abnormal growth and proliferation. Certain organic acids, such as 2-hydroxyglutarate and citrate, are reported as inhibitors of TET2. Hence, these organic acids, including 2-hydroxyglutarate and citrate, are suggested to potentiate the growth and proliferation of cancer cells [23-31].

Based on the above understating and impending gaps in OSMF-OSCC, we present a novel approach to the preparation, purification, filtration, and analysis of SABFI by vertical tube gel electrophoresis (VTGE) and liquid chromatography-high resolution mass spectrometry (LC-HRMS). To investigate the potential of SABFI-derived organic acids in promoting OSMF-OSCC, particularly their role as inhibitors of the TET2 epigenetic modifier, we employed both in vitro and in silico techniques.

MATERIALS AND METHODS

Collection of saliva and BQ

Saliva from healthy subjects aged 30 to 50 was collected as per the Institutional ethics committee approval of Dr. D. Y. Patil Vidyapeeth, Pune and informed consent was collected (approval code: Ref.No.DYPV/EC I 14). The recruited human subjects had no history of tobacco chewing or smoking. BQ was procured in the local market.

Preparation of SABFI

For the preparation of SABFI, 0.5 mg of BQ was mixed and grinded with 1 mL of saliva. Here, the saliva of the healthy control was centrifuged at 5,000 × *g* for 20 minutes to get rid of debris and clear saliva was obtained for SABFI preparation. The BQ-saliva mixture was then vortexed for 10 minutes. Next, BQ-saliva amalgamation was centrifuged at 10,000 × *g* in two cycles for 30 minutes to obtain a final clear supernatant. Finally, BQ-saliva amalgamated supernatant was filtered using a 0.45-micron filter membrane to obtain SABFI. Furthermore, SABFI was estimated by weight/volume analysis, and a 3 mg/mL stock of SABFI was prepared and stored at –20°C for further investigation and cell-based assays. As a control, saliva without BQ was processed and prepared for analysis and cell-based assays [32].

VTGE-assisted purification SABFI

For the purification and identification of SABFI components, we employed an in-house developed VTGE system. In brief, VTGE used 15% (acrylamide: bis, 29:1) gel to exclude large macromolecules such as proteins, polysaccharides, lipids, and other chemicals from SABFI. The details of the running conditions of VTGE and procedure were adopted from the previously published in-house developed protocol [33,34]. A flow model of the VTGE-assisted procedure is illustrated in Figure S1. At the end of VTGE-assisted purification of SABFI, purified organic acids of SABFI were collected and stored at –20°C for further analysis by LC-HRMS. In brief, the LC component consisted of the Zorbax RP-C18 column with 2.1 × 50 μm dimensions. The salivary and SABFI metabolites identifications were carried out in a positive electrospray ionization (ESI) M-H mode. The mass spectrometer component was quadrupole time-of-flight mass spectrometer (Q-TOF-MS) (6,500 Series Q-TOF LC/MS system; Agilent Technologies) in dual Jet Stream Technology Ion Source ESI mode. A detailed protocol was adopted from a previously published procedure [34].

Effects of SABFI on oral cancer cells

To evaluate the effects of saliva control and SABFI, the oral cancer cell line KB-31 was maintained in complete Dulbecco's modified Eagle medium (DMEM) high glucose medium supplemented with 10% FBS penicillin (100 units/mL)/streptomycin (100 μg/mL) at 37°C in a humidified 5% CO_2

incubator. Oral cancer cells were plated into six-well plates at a density of 150,000 cells per well. After 16 to 18 hours of overnight growth, complete DMEM medium with saliva (5 μL) and SABFI (10 μg/mL) were added in triplicate in respective wells of the six-well plate. Incubation of oral cancer cells with SABFI was allowed for 120 hours, and cells were observed afterward. The morphology of cells was studied with the help of routine phase contrast microscopy. Then, oral cancer cells were harvested and collected using the standard procedure. A typical trypan blue dye exclusion assay was performed to determine the total and viable cells.

Furthermore, the above-prepared oral cancer cell suspension was estimated for early apoptosis using dual staining by ethidium staining and acridine orange. In short, 10 μL of cell suspension containing 500 cells was mixed with 10 μL of staining reagent (ethidium bromide and acridine orange). A detailed procedure for dual staining is adapted from a previously published procedure [33,34]. A fluorescence microscopy image was collected with the help of suitable green and red filters.

Measurement of cell viability

Oral cancer cells were plated into 96-well plates at a density of 10,000 cells per well. After 16 to 18 hours of overnight growth, complete DMEM medium with saliva (5 μL) and SABFI (10 μg/mL) were added in triplicate in respective wells of the six-well plate. Incubation of oral cancer cells with SABFI was allowed for 120 hours. Then, oral cancer cells were harvested and collected using the standard procedure. A routine MTT assay was performed to determine the viability and adapted from a previously published procedure [33,34].

Cell cycle analysis

Oral cancer cells were plated into six-well plates at a density of 150,000 cells per well. After 16 to 18 hours of overnight growth, complete DMEM medium with saliva (5 μL) and SABFI (10 μg/mL) were added in triplicate in respective wells of the six-well plate. Incubation of oral cancer cells with SABFI was allowed for 120 hours. At the end of treatment, cells were harvested for cell cycle analysis by propidium iodide (PI) staining assay adapted from a previously published procedure [33,34]. In brief, harvested cells were fixed with the help of cold 70% ethanol. Next, washed twice with PBS and followed by centrifugation to obtain cell pellets. Then, 50 μL of a 100 μg/mL stock of RNase and 200 μL PI (from 50 μg/mL stock solution) was added to the cell pellets. Finally, measurements of PI-stained cells were recorded with the help of a BD Jazz Flow cytometer BD (Biosciences) and a suitable bandpass filter.

Molecular docking

The SABFI-derived organic acids were identified by LC-HRMS. These organic acids including citric acid (PubChem CID: 311), malic acid (PubChem CID: 525), fumaric acid (PubChem CID: 444972), 2-methylcitric acid (PubChem CID: 515), 2-hydroxyglutarate (PubChem CID: 53262286), *cis*-aconitic acid (PubChem CID: 643757), succinic acid (PubChem CID: 160419), 2-hydroxyglutaric acid lactone (PubChem CID: 251524), tartaric acid (PubChem CID: 444305), β-ketoglutarate (β-KG) (PubChem CID: 68328) and α-KG, a known substrate of TET2 (PubChem CID: 164533) were selected as potential ligands for molecular docking to evaluate the inhibitory potential against TET2 (tes, protein data bank [PDB] ID: 5D9Y). Further, sdf files of these organic acids were downloaded from the PubChem database. The crystal structures of TET2 (PDB ID: 5D9Y) were downloaded from the research collaboratory for structural bioinformatics PDB database. Target proteins and ligands, downloaded from the PDB and other databases were pre-processed before docking using AutoDock Tools [35,36]. Processed PDB files were saved as protein data bank, partial charge (Q), and atom type (T) format input files for docking by AutoDock Vina [36]. Apart from this, we considered α-KG (PubChem CID: 164533) as a known substrate of TET2 as a positive control to evaluate the competitive inhibitory binding by SABFI-derived organic acids. Furthermore, we visualized SABFI derive organic acids and TET2 complexes with the help of Discovery Studio Visualizer [37]. The key inhibitory amino acid residues of TET2 interacting with potential organic acids were recorded and imaged in holistic and 3-dimensional interaction patterns.

Molecular dynamics simulations

Based on the above molecular docking date on the specific binding by SABFI-derived organic acids, citrate showed the equivalent binding affinity and also shared inhibitory pocket amino acid residues. Hence, we used Desmond software for 20 ns molecular dynamics (MD) simulation of complexes of TET2-citrate and TET2-α-KG, a known substrate of TET2 to confirm the binding stability and strength of the complex [38]. Desmond software includes adding pressure, temperature, volume system, and many other functions to complete the protein-ligand binding [39]. The protein-ligand complex was immersed in a water-filled orthorhombic box of 10 Å spacing. The target ligand-protein complex had 21,066 water molecules using an extended three-point water model (TIP3P) with periodic boundary conditions. These studies were performed with a run of 20 ns and temperature 300 K, considering specific parameters such as integrator as MD. The conformational changes upon binding of organic acids with TET2 were recorded with the help of 1,000 trajectory frames generated during 20 ns MD simulation. Root mean square deviation (RMSD) and root mean square fluctuations (RMSF) were calculated to confirm the deviation and fluctuations in the conformation of the organic acids-TET2 complex [39].

RESULTS

Identification of SABFI-derived organic acids

The LC-HRMS analysis revealed a set of organic acids derived from SABFI such as citric acid. malic acid, fumaric acid, 2-methylcitric acid, 2-hydroxyglutarate, *cis*-aconitic acid, succinic acid, 2-hydroxyglutaric acid lactone, tartaric acid, and β-ketoglutaric acid (Table 1). These organic acids identified in SABFI were normalized over saliva control. Among these identified organic acids, retention time ranged from 0.717 to 0.867 minutes. It is important to note that all these organic acids showed good abundance in SABFI compared to saliva control, with matching scores of more than 83.06 to 99.61. The abundance in arbitrary unit 194,324, 721,504, and 158,991 was found to be for first three chemicals such as citric acid, malic acid, and fumaric acid, respectively. The

Table 1. List of organic acids found in SABFI after normalized over saliva control by employing a novel and in-house VTGE and LC-HRMS

Sr. No.	Name of SABFI oncometabolites	Chemical formula	RT	m/z	Mass	Score	Abundance (AU)
1	Citric acid	C6 H8 O7	0.826	191.0201	192.0273	99.01	1,943,241
2	L-malic acid	C4 H6 O5	0.826	133.0143	134.0216	99.61	721,504
3	Fumaric acid	C4 H4 O4	0.826	115.0034	116.0106	98.8	158,991
4	2-methylcitric acid	C7 H10 O7	0.842	205.0349	206.0422	84.52	62,048
5	2-hydroxyglutarate	C5 H8 O5	0.842	147.0296	148.0369	83.06	49,219
6	*cis*-aconitic acid	C6 H6 O6	0.834	173.0092	174.0164	85.81	39,745
7	Succinic acid	C4 H6 O4	0.867	117.0192	118.0263	90.72	33,758
8	2-hydroxyglutaric acid lactone	C5 H6 O4	0.717	129.0193	130.0265	85.58	27,519
9	Tartaric acid	C4 H6 O6	0.726	149.0088	150.0161	83.99	15,087
10	β-ketoglutaric acid	C5 H6 O5	0.842	145.0143	146.0217	83.75	12,681

SABFI, saliva-amalgamated betel quid filtrate; VTGE, vertical tube gel electrophoresis; LC-HRMS, liquid chromatohgraphy-high resolution mass spectrometry; RT, retention time; m/z, mass/charge; AU, arbitrary unit.

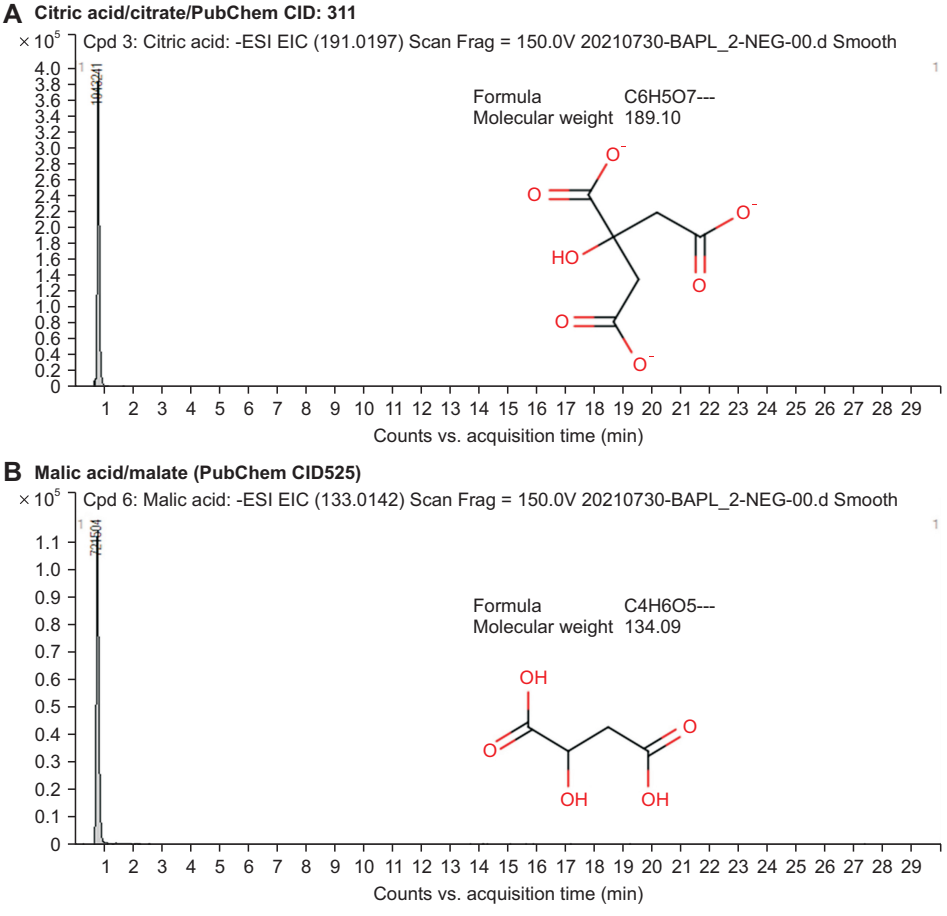

Figure 1. LC-HRMS profiling of SABFI-derived organic acids show the abundance of citric acid and malic acid. EIC of citric acid and malic acid in negative mode ESI spectra of SABFI purified by VTGE. LC-HRMS, liquid chromatography-high resolution mass spectrometry; SABFI, saliva-amalgamated betel quid filtrate; EIC, extracted ion chromatogram; ESI, electrospray ionization; VTGE, vertical tube gel electrophoresis.

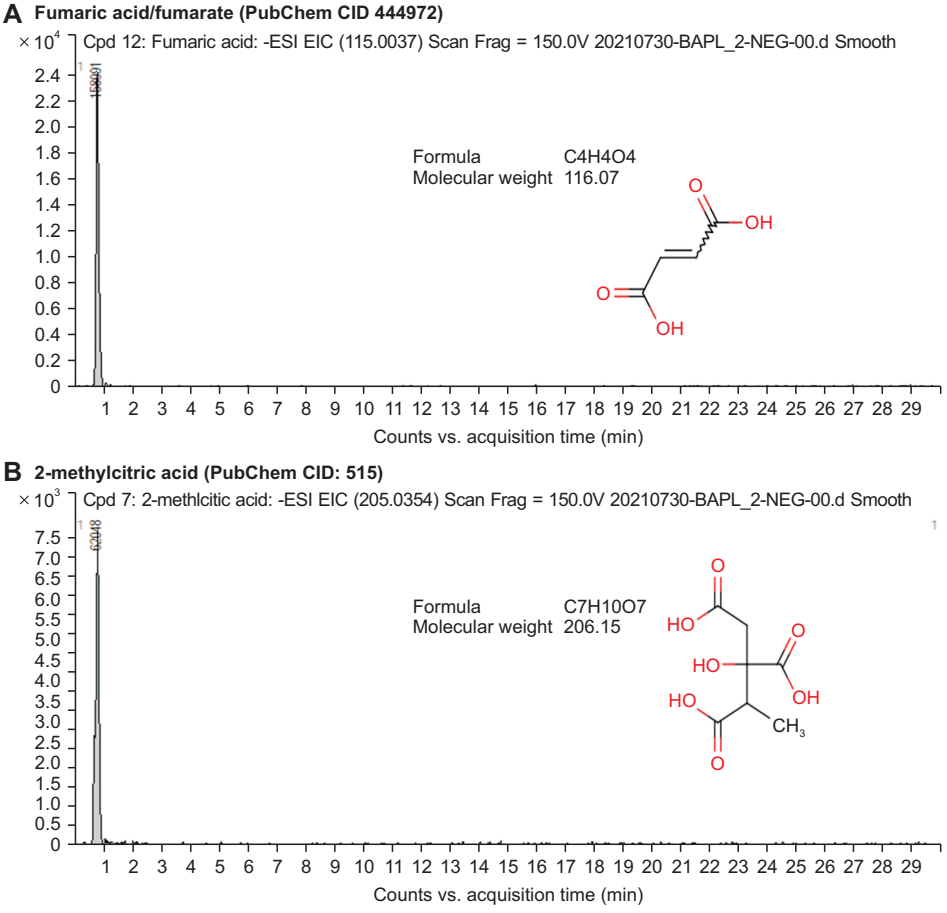

Figure 2. SABFI-derived organic acids indicate the abundance of fumaric acid and 2-methylcitric acid. EIC of fumaric acid and 2-methylcitric acid in negative mode ESI spectra of SABFI purified by VTGE. SABFI, saliva-amalgamated betel quid filtrate; EIC, extracted ion chromatogram; ESI, electrospray ionization; VTGE, vertical tube gel electrophoresis.

extracted ion chromatogram of purified SABFI collected in negative ESI mode revealed the abundance and molecular characteristics of identified representative organic acids such as citric acid and L-malic acid (Fig. 1), and fumaric acid and 2-methylcitric acid (Fig. 2), 2-hydroxyglutarate and *cis*-aconitic acid (Fig. 3).

In line with our findings, organic acids such as citric acid, malic acid, fumaric acid, 2-methylcitric acid, 2-hydroxyglutarate, succinic acid, 2-hydroxyglutaric acid lactone, and α-ketoglutaric acid are directly or indirectly linked with the altered regulation of metabolic pathways in various types cancer cells [13-28,40-45]. In recent, noticeable metabolic profiling of biological fluids and tumor tissues suggested the enhanced levels of metabolites such as citric acid, malic acid, fumaric acid, 2-methylcitric acid, 2-hydroxyglutarate, *cis*-aconitic acid, succinic acid, and 2-hydroxyglutaric acid lactone [40-45]. Therefore, it is highly reasonable that SABFI that is prepared from BQ will have an abundance of these organic acids due to varied mixtures of areca nut, betel leaf, sweeteners, flavoring agents, and other forms of plant-derived mixtures.

Existing findings suggest the highly variable (1 to 100 ng/mL) levels of AN and various forms of BQ-derived chemicals such as guvacoline and arecoline in the expectorated saliva of chewers. Various explanations are extended, including the various compositions of BQ and fresh AN that may differ based on socioeconomic and demographic factors. However, it is essential to note that existing methodologies for these earlier reports significantly differ, specifically in the collection of BQ-saliva expectorant, preparation, and extraction of chemicals such as guvacoline and arecoline. Most of these methods used organic solvent-based extraction of guvacoline and arecoline, which may be one of the reasons for the significant variation and possibly overestimation of guvacoline and arecoline in saliva over biologically abundant in the saliva environment. In essence, after the preparation of BQ-saliva expectorant, the supernatant should have been centrifuged twice at high speed to get rid of immiscible BQ/AN derived particle, followed by the 0.45-micron syringe filter-based filtration to obtain a completely clear supernatant of BQ-saliva expectorant/amalgamation. Because BQ/AN-derived chemicals, such as guvacoline and arecoline, are alkaloids, they are nearly miscible in the saliva's alkaline pH, which typically ranges from 8.2 to 8.4. During the preparation of BQ-saliva expectorant, it is essential to exclude the presence of immiscible BQ/AN particles to avoid overestimating chemicals such as guvacoline and arecoline.

To address these limitations that are observed in the BQ/AN-saliva expectorant, we have employed an in vitro meth-

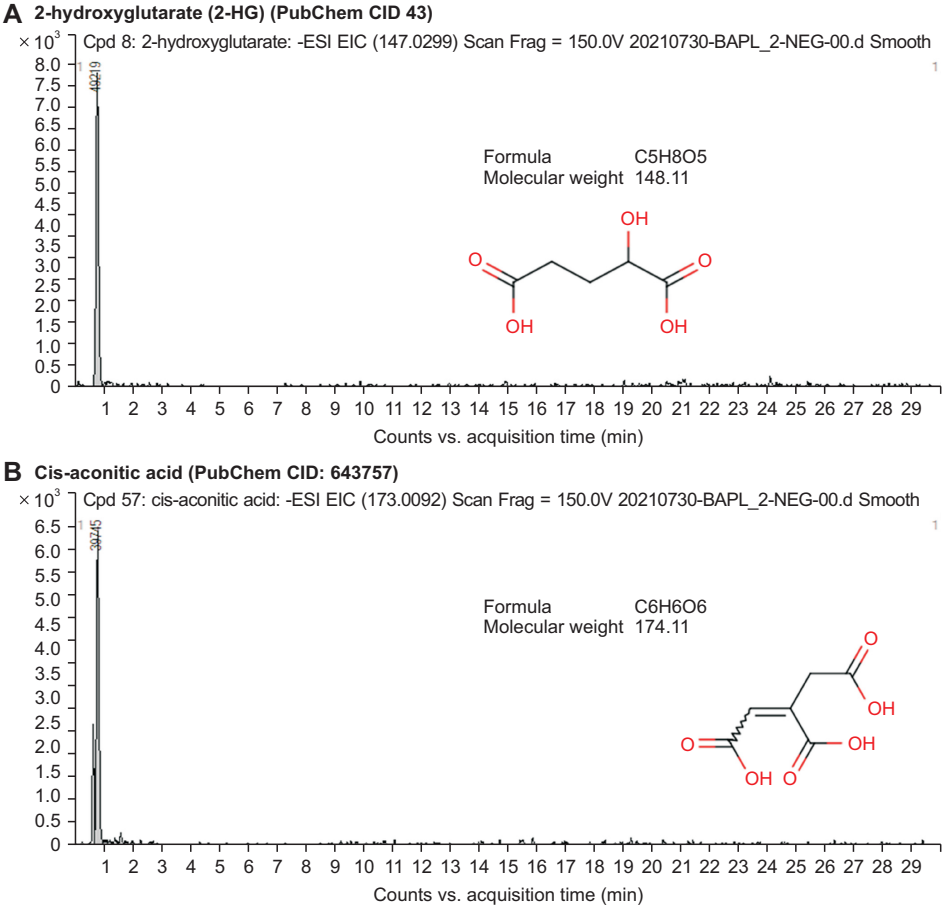

Figure 3. Profiling of SABFI-derived organic acids depict presence of 2-hhydroxyglutarate and *cis*-aconitic acid. EIC of 2-hhydroxyglutarate and *cis*-aconitic acid in negative mode ESI spectra of SABFI purified by VTGE. SABFI, saliva-amalgamated betel quid filtrate; EIC, extracted ion chromatogram; ESI, electrospray ionization; VTGE, vertical tube gel electrophoresis.

odology with the preparation of BQ-saliva amalgamation, followed by centrifugation and filtration through a 0.45-micron syringe filter to obtain SABFI. Later on, SABFI has been used for LC-HRMS based identification of organic acids. Our observations did not detect guvacine and arecoline in SABFI, even at concentrations of 1 to 10 ng/mL. We conclude that no detection of guvacine and arecoline in SABFI may be due to the limitation of sensitivity of the used approach. Nevertheless, our observations align with the earlier reports [5-8] that the level of guvacine and arecoline in the AN-saliva expectorant is low, ranging from 1 ng to 10 ng/mL. Our experiment used BQ, which potentially has a lower amount of AN than AN alone, and BQ is added with other flavoring agents, sweeteners, mouth fresheners, and other compounds. Hence, a low level of less than 1 ng of guvacine and arecoline in the SABFI could be the reason for non-detection in our approach.

SABFI-induced proliferative arrest in oral cancer cells

Next, BQ-derived SABFI containing these organic acids were evaluated for their effects on oral cancer cells. A simple and reliable trypan blue dye exclusion assay suggests that exposure of SABFI to oral cancer cells leads to the arrest of growth and proliferation by up to 55% (Fig. 4A and 4B). Similarly, the MTT assay indicated that the viability of oral cancer cells was reduced by up to 77.38% after normalization over saliva control (Fig. 5A and 5B). It is important to note that we did not find significant cell death and toxicity due to SABFI compared to saliva control. Furthermore, we estimated the presence of early apoptosis in oral cancer cells using an acridine orange/ethidium bromide dual staining assay. The data indicated the presence of more than 60% early apoptosis in oral cancer cells treated by SABFI over saliva control (Fig. 6A and 6B).

Given the observed proliferative arrest and signs of early apoptosis, we performed cell cycle analysis by PI staining. Data indicated significant level of early apoptotic cell death in oral cancer cells treated by SABFI (Fig. 7A and 7B). Cell cycle distribution indicated that SABFI did not alter the G_0/G_1 S and GM-M phase duration over saliva control. Interestingly, the proportion of oral cancer cells treated by SABFI demonstrated significant elevation of with hypodiploid DNA content (or early apoptotic cells) in cell cycle distribution. Our observations were in agreement with existing findings that some of chemicals and anticancer compositions may induce proliferation arrest and early apoptotic cell death in cancer cells [38,40,41,46-49].

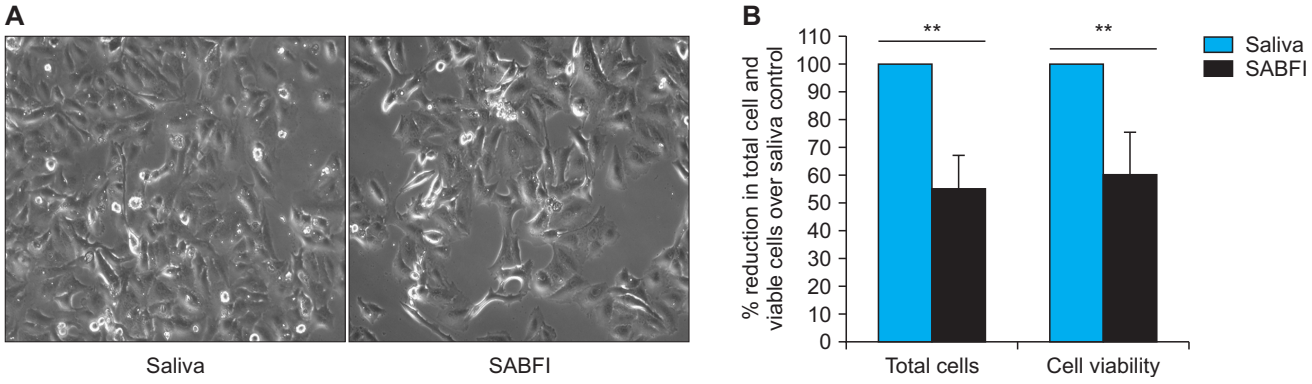

Figure 4. Reduced proliferation in oral cancer cells treated by SABFI. (A) Oral cancer cells were treated by saliva control and SABFI (10 μg/mL) for 72 hours. Routine microscopy was performed at 100× to observe the cell number and cellular morphology. (B) Oral cancer cells were treated by saliva control and SABFI (10 μg/mL) for 72 hours. The percentage cell viability of oral cancer cells was estimated by the trypan blue dye exclusion assay. Trypan blue dye exclusion assay was performed to estimate viable and dead cells. Data are represented as mean ± SD. Each experiment was conducted independently three times. SABFI, saliva-amalgamated betel quid filtrate. **Significantly different from the saliva control at *P*-value ≤ 0.01.

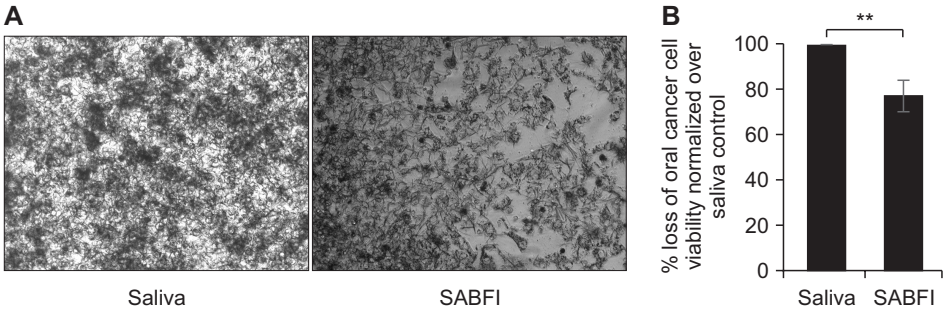

Figure 5. Reduction in total viable oral cancer cells exposed to SABFI. (A) Oral cancer cells were treated by saliva control and SABFI (10 μg/mL) for 72 hours. A routine MTT assay was performed at the end of treatment. Routine microscopy was performed at 100× to observe the cellular morphology and cell number. (B) Oral cancer cells were treated by saliva control and SABFI (10 μg/mL) for 72 hours. The percentage total viable of oral cancer cells was estimated by normalizing over saliva control. Data are represented as mean ± SD. Each experiment was conducted independently three times. SABFI, saliva-amalgamated betel quid filtrate. **Significantly different from the saliva control at *P*-value ≤ 0.01.

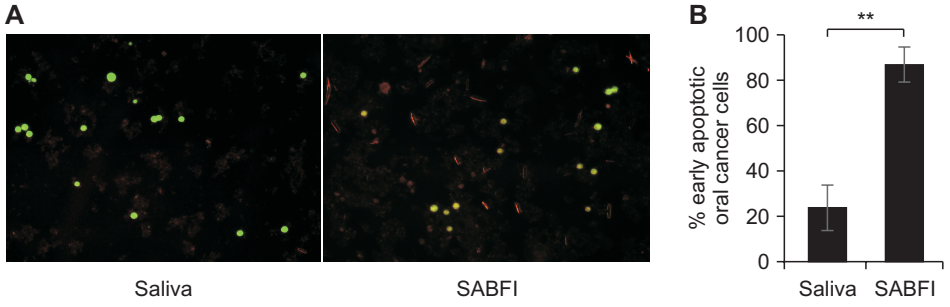

Figure 6. Presence of early apoptosis in oral cancer cells treated by SABFI-derived organic acids. (A) Oral cancer cells were treated by saliva control and SABFI (10 μg/mL) for 120 hours. Dual staining by acridine orange and ethidium bromide was performed at the end of the treatment. Routine microscopy was performed at 100× to observe the differential staining by acridine orange and ethidium bromide to estimate early apoptotic cells. (B) Oral cancer cells were treated by saliva control and SABFI (10 μg/mL) for 72 hours. Early apoptotic cells showed yellow-green fluorescence by acridine orange staining of nucleus and concentrated into crescent or granular that is located in one side of the cells. Late apoptotic cells showed orange florescence of nucleus by ethidium bromide staining and gathered in concentration. Necrotic cells displayed increased volume and uneven orange red fluorescence and appears dissolved or near disintegrated. The percentage of early apoptotic oral cancer cells was estimated by normalizing over saliva control. Data are represented as mean ± SD. Each experiment was conducted independently three times. SABFI, saliva-amalgamated betel quid filtrate. **Significantly different from the saliva control at *P*-value ≤ 0.01.

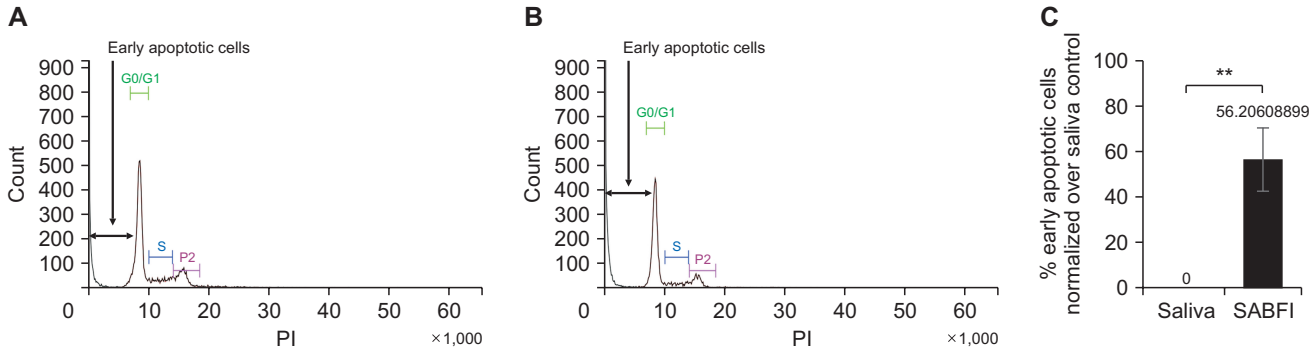

Figure 7. SABFI-derived organic acids induce early apoptotic cell death in oral cancer cells. (A) Oral cancer cells were treated by saliva control and SABFI (10 μg/mL) for 120 hours. At the end of treatment, PI-stained oral cancer cells were analyzed by flow cytometry. (B) Oral cancer cells were treated by saliva control and SABFI (10 μg/mL) for 72 hours. The percentage of early apoptotic cell death was calculated by normalizing over saliva control. Data are represented as mean ± SD. Each experiment was conducted independently three times. SABFI, saliva-amalgamated betel quid filtrate; PI, propidium iodide. **Significantly different from the saliva control at *P*-value ≤ 0.01.

We observed a significant presence of early apoptosis, while conventional cell death, as observed in the case of genotoxic agents, was not evident. These findings prompted us to hypothesize that the organic acids derived from BQ could potentially induce alterations in the metabolic landscape of oral cancer cells, beyond exerting cellular toxicity. This observation suggests that intracellular levels of SABFI-derived organic acids in oral cancer cells might disrupt certain metabolic-epigenetic pathways. This proposition is based on the known associations between these organic acids, such as citric acid, α-KG, 2-hydroxyglutarate, fumaric acid, succinic acid, and malic acid, and changes in metabolic and epigenetic pathways [38,40,41,46-49].

Earlier data on AN extract with doses ranging from 10 μg to 400 μg/mL showed only cell cycle arrest in oral KB cells and other types of cells, with a noticeable decrease in the duration of S-phase [38,40,48,49]. Interestingly, existing data did not indicate the apparent presence of cell death, including apoptotic cell death and toxicity. Similarly, SABFI containing significant amounts of organic acids such as citric acid, β-KG, malic acid, 2-hydroxyglutarate, succinic acid, and fumaric acid caused cell cycle arrest in oral KB cells and a significant decrease in S-phase that was compensated for by an increase in Sub-G_1 phase compared to saliva control.

Therefore, our observations align with the current views that AN extract or BQ-derived extract containing various forms of organic acids may induce cell cycle arrest in exposed oral KB cells. Such observations emphasize the possibilities of alterations in the cellular landscape of SABFI-exposed cells beyond the routine genotoxicity in the form of metabolic-epigenetic changes.

Molecular docking and MD simulations

Based on our observations and supported by the existing views, we started to screen various epigenetic modifiers such as DNA demethylases and histone demethylases [46,47,50-58]. Initial screening data is not shown. Based on the initial data, we focused on the TET2, a form of DNA demethylase known to be involved in the DNA repair response gene and act as a tumor suppressor. We hypothesized that SABFI-derived organic acids would inhibit TET2 and, as a result, block the DNA repair response in oral cancer cells during endogenous and exogenous chemical exposure while using BQ.

Molecular docking data provided interesting observations that SABFI-derived citric acid, β-KG, 2-hydroxyglutarate, fumaric acid, succinic acid, and malic acid showed a strong affinity to act as a competitive inhibitor of α-KG, the natural substrate of TET2 during catalytic demethylase activity (Table 2). Further, visualization of the docked complex of β-KG-TET2 (Fig. 8A and 8C) and citrate-TET2 (Fig. 9A and 9C) revealed the overlapping key amino acid residues, including ARG1261 compared to α-KG, the natural substrate of TET2 (Fig. 8B and 8D). The TET2 binding affinity of citrate (–6.1 kcal/mol), β-KG (–5.7 kcal/mol), 2-hydroxyglutarate (–5.5 kcal/mol), fumaric acid (–5.1 kcal/mol), succinic acid (–5.0 kcal/mol), and malic acid (–5.0 kcal/mol) found to be highly similar to α-KG, the natural substrate of TET2. The number of hydrogen bonds between SABFI-derived organic acids, and TET2 ranged from 3 to 6, with bond distances in the range of 2.0 to 3.5 Å that are competitive over α-KG, the natural substrate of TET2 (Table 2). These data helped us to further strengthen the claim in terms of the stability of the organic acids-TET2 complex by using MD simulations. The visualization of the organic acids-TET2 complex revealed that crucial amino acid residues such as ARG1261, HIS1382, HIS1416, HIS1881, ARG1896, and SER1898 are responsible for the inhibitory binding, as ARG1261, HIS1416, HIS1382, and HIS1881 have previously been reported for interactions with a known TET2 substrate α-KG for demethylase activity.

To study conformational stability, MD simulations of citrate and β-KG against TET2 were performed in a 20 ns frame. The RMSD plots of the β-KG-TET2 complex (Fig. 10A) and the citrate-TET2 complex (Fig. 10B) revealed the acceptable range of RMSD values for the 20 ns frame, ranging from 1.5

Table 2. SABFI derived organic acids are predicted as inhibitors of TET-2 enzyme

Sr. No.	Name of polyamines/ligands with their PubChem CIDs	Binding energy (–kcal/mol)	Inhibitory site binding resides	No. of hydrogen bonds	Distance of hydrogen bonds (Å)
1	Citric acid (PubChem CID: 311)	–6.1	HIS1881 ARG1261 ARG1896 HIS1382 HIS1416 SER1898	6	2.03 2.30 2.36 2.20 2.77 2.22
2	Malic acid (PubChem CID: 525)	–5.0	HIS1881 ARG1261 HIS1416 HIS1382 SER1898 ARG1896	6	1.93 2.27 2.20 2.93 2.26 2.47
3	Fumaric acid (PubChem CID: 444972)	–5.3	ARG1261 HIS1881 ARG1896 HIS1382 SER1898	5	2.07 1.98 2.26 2.10 2.44
4	2-methylcitric acid (PubChem CID: 515)	–5.3	ARG1261 THR1372 TRY1902 SER1290 HIS1386 HIS1904	6	2.32 2.23 2.40 2.90 2.92 2.99 3.02
5	2-hydroxyglutarate (PubChem CID: 53262286)	–5.5	ARG1896 SER1898 ARG1261 ASP1384 CYS1374 ARG1261	6	1.99 1.95 2.30 2.32 2.36 2.71
6	*cis*-aconitic acid (PubChem CID: 643757)	–6.2	ARG1261 SER1898 ARG1896 ASP1384 HIS1881 HIS1416	6	1.91 1.95 2.08 2.32 2.43 2.56
7	Succinic acid (PubChem CID: 160419)	–5.0	ARG1261 HIS1881 ARG1896 HIS1382 SER1898	5	2.07 1.94 2.26 2.11 2.17
8	2-hydroxyglutaric acid lactone (PubChem CID: 251524)	–5.4	ARG1261 HIS1382 HIS1416	3	2.20 2.21 2.62
9	Tartaric acid (PubChem CID: 444305)	–5.2	ARG1261 SER1286 THR1372 ASN1387	6	2.17 2.35 2.41 2.58 2.73 2.78
10	β-ketoglutarate (PubChem CID: 68328)	–5.5	HIS1416 ARG1896 SER1898 CYS1374 ARG1261	5	1.98 3.72 1.97 2.15 2.56
11	α-ketoglutarate, a known substrate of TET-2 (PubChem CID: 164533)	–5.7	HIS1881 HIS1382 ARG1261 HIS1416	4	1.98 2.01 2.21 2.02

The binding affinity and nature of inhibitory site amino acid residues are analyzed with the help of AutoDock Vina and Discovery studio software. SABFI, saliva-amalgamated betel quid filtrate; TET-2, Ten-Eleven Translocation-2.

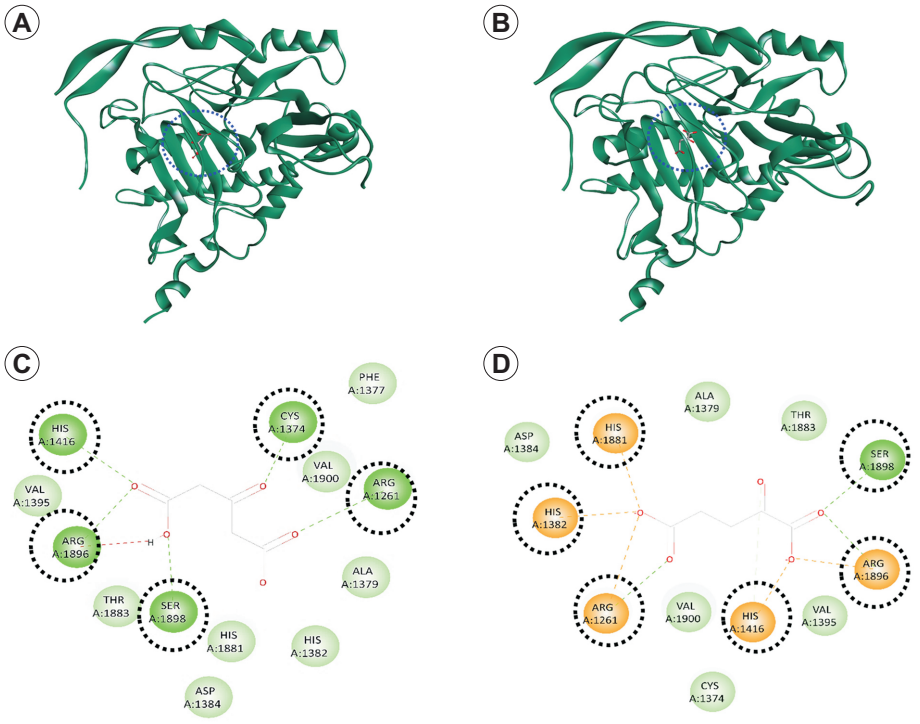

Figure 8. SABFI-derived oncometabolite β-KG shows competitive inhibitory effects upon TET2 in place of α-KG, a natural substrate. Molecular docking and inhibitory interaction by β-KG and α-KG upon TET2 was studied with the help of AutoDock Vina. (A) A ribbon structure with a full 3-dimensional (3D) view between β-KG and TET2. (B) A ribbon structure with a full 3D view between α-KG and TET2. (C) Discovery Studio Visualizer assisted 2D image of docked molecular structure between β-KG and TET2. (D) Discovery Studio Visualizer assisted 2D image of docked molecular structure between α-KG and TET2. SABFI, saliva-amalgamated betel quid filtrate; β-KG, β-ketoglutarate; TET2, Ten-Eleven Translocation-2.

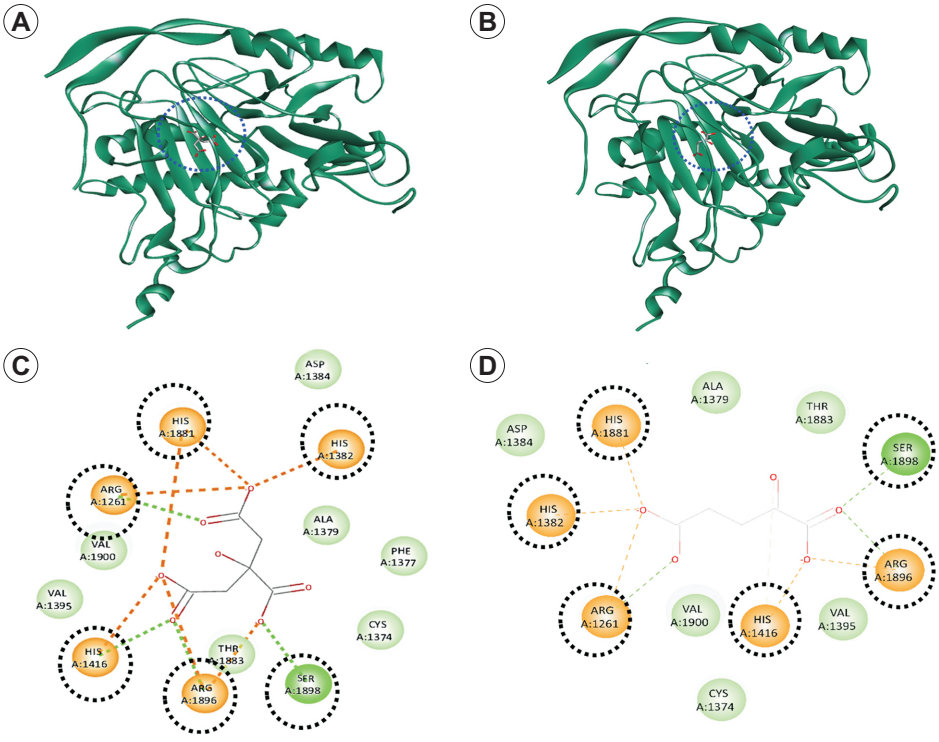

Figure 9. SABFI-derived oncometabolite citrate displays competitive inhibitory binding to TET2 against α-KG, a natural substrate. Molecular docking and inhibitory interaction by citrate and α-KG upon TET2 was studied with the help of AutoDock Vina. (A) A ribbon structure with a full 3-dimensional (3D) view between citrate and TET2. (B) A ribbon structure with a full 3D view between α-KG and TET2. (C) Discovery Studio Visualizer assisted 2D image of docked molecular structure between citrate and TET2. (D) Discovery Studio Visualizer assisted 2D image of docked molecular structure between α-KG and TET2. SABFI, saliva-amalgamated betel quid filtrate; α-KG, α-ketoglutarate; TET2, Ten-Eleven Translocation-2.

to 3.5. It is worth noting that at the end of both citrate and β-KG simulations, the RMSD values appeared to be stable, with no increase or decrease in the RMSD of TET2 protein (Fig. 10A and 10B).

RMSF plots of citrate and β-KG against TET2 revealed the most negligible fluctuations of TET2 conformations as indicated in the amino acid residues (x-axis), with RMSF values ranging from 0.5 to 2.5 (Fig. 11A and 11B, respectively). There are some apparent fluctuations in the region of TET2 polypeptide due to the presence of the bridge sequence. On

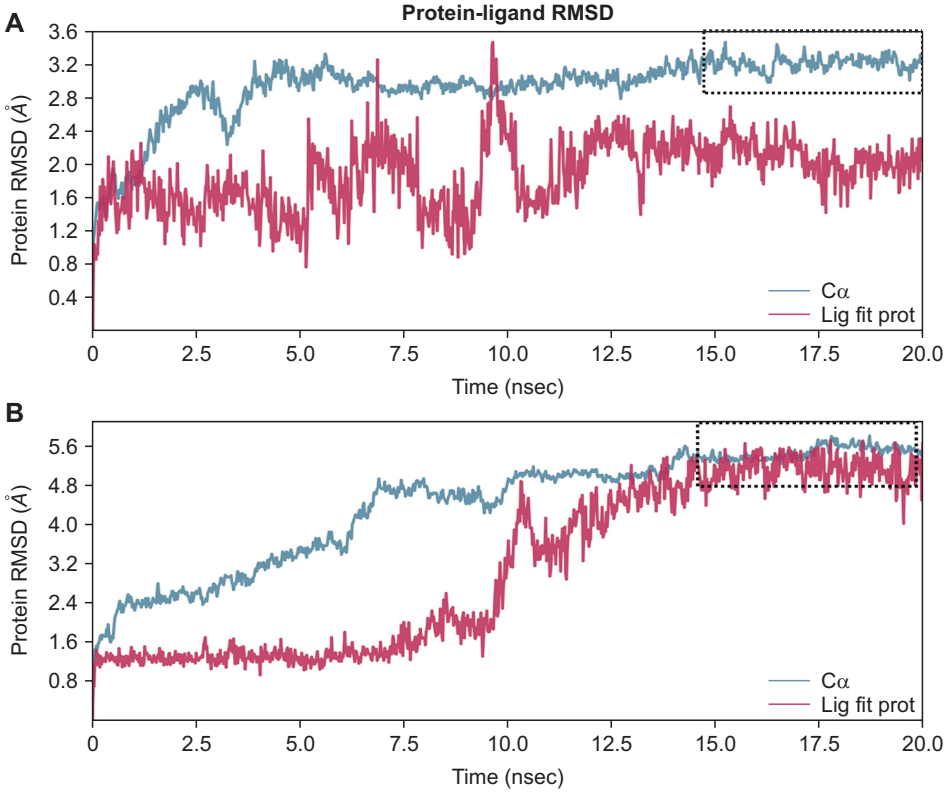

Figure 10. TET2 RMSD plot shows stable inhibitory complex with organic acids. MD simulations for 20 ns derived RMSD plot of c-Raf kinase in complex with (A) β-KG-TET2 (A) and (B) citrate-TET2 (B). Cα denotes the protein RMSO plot on X-axis. Lig fit prot shows the RMSD of a ligand when the protein-ligand complex is first aligned on the protein backbone of the reference and then the RMSD of the ligand heavy atoms is measured. TET2, Ten-Eleven Translocation-2; RMSD, root mean square deviation; MD, molecular dynamic; β-KG, β-ketoglutarate.

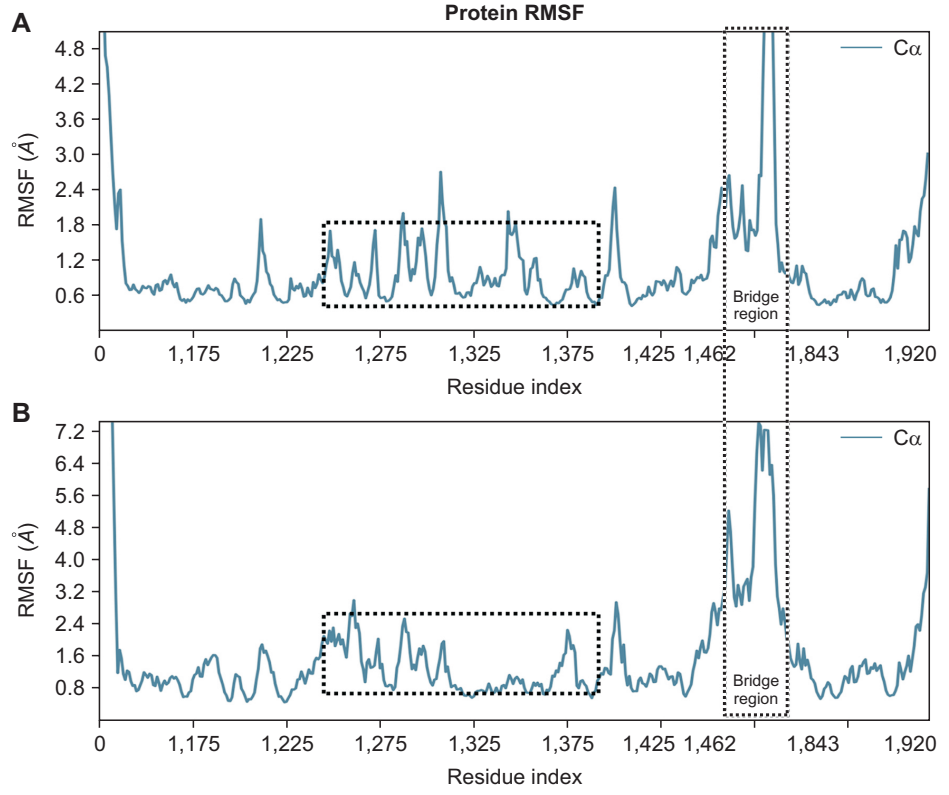

Figure 11. RMSF plot of organic acids-TET2 complex displays least fluctuations of inhibitory amino acid interacting residues. MD simulations for 20 ns derived RMSF plot of TET2 in complex with (A) β-KG-TET2 (A) and (B) citrate-TET2 (B). RMSF, root mean square fluctuation; TET2, Ten-Eleven Translocation-2; MD, molecular dynamic; β-KG, β-ketoglutarate.

the other hand, the inhibitory binding residues ARG1261 to HIS1416, on the other hand, had no significant RMSF values for the citrate-TET2 and β-KG-TET2 complexes.

Data show protein-ligand contact maps of TET2-KG and TET2-citrate interactions, with interaction fractions ranging from 0.5 to 1.2 for important residues such as ARG1261, HIS1382, HIS1416, HIS1881, ARG1896, and SER1898 (Fig. 12A and 12B). The nature of the interacting forces responsible for TET2-oncometabolite stability encompasses bonds such as hydrogen bonds, and hydrophobic, ionic, and water bridges. When the RMSD, RMSF, and protein-ligand contact plots were combined, they strongly suggested that organic acids like citrate and α-KG could be a potent competitive inhibitor of TET2 in place of the natural substrate α-KG.

Data suggest that TET proteins contribute to maintaining active DNA demethylation [13-18]. These DNA demethylases, including TET2, are known as oxygenases that catalyze the conversion of hydroxylate 5-methylcytosine (5-mC) into 5-hydroxymethylcytosine (5-hmC). Further, 5-hmC is oxidized into 5-formylcytosine (5-fC) and 5-carboxylcytosine (5-caC) by associated proteins [19-22]. In the end, base excision repair (BER) proteins help to remove 5-fC, and 5-caC is replaced with regular cytosine. Furthermore, TET2 is responsible for controlling the transcription of selected target genes, including DNA damage repair proteins and cell cycle proteins. [23-27] However, a significant gap in the literature addresses the link between SABFI-derived organic acids and TET2 inhibition, which could induce proliferation arrest in exposed oral cancer cells and eventually lead to further genomic instability.

DISCUSSION

Our findings on SABFI-derived organic acids as potential inhibitors of TET2 agree with current views on the metabolic-epigenomic axis in cancer cells [13-18]. Findings suggest a high accumulation of fumarate and succinate in cancer cells [30-37,39,50-53]. Fumarate and succinate are suggested for their inhibitory effects upon DNA demethylases and histone demethylases lysine-specific demethylase 4A (KDM4A) and KDM4B. Therefore, the presence of fumarate and succinate in SABFI could be proposed for their interference with the TET2 enzyme.

In another finding, 2-hydroxyglutarate and its lactonized products such as 2-hydroxyglutarate-γ-lactone are elevated due to somatic mutations in the isocitrate dehydrogenase gene [30,31]. Organic acids such as 2-hydroxyglutarate and its lactonized product 2-hydroxyglutarate-γ-lactone are considered organic acids potentially inhibiting TET2 and histone demethylases [35-37,39,50-52]. Therefore, the inhibitory potential of 2-hydroxyglutarate is related to its ability to alter the

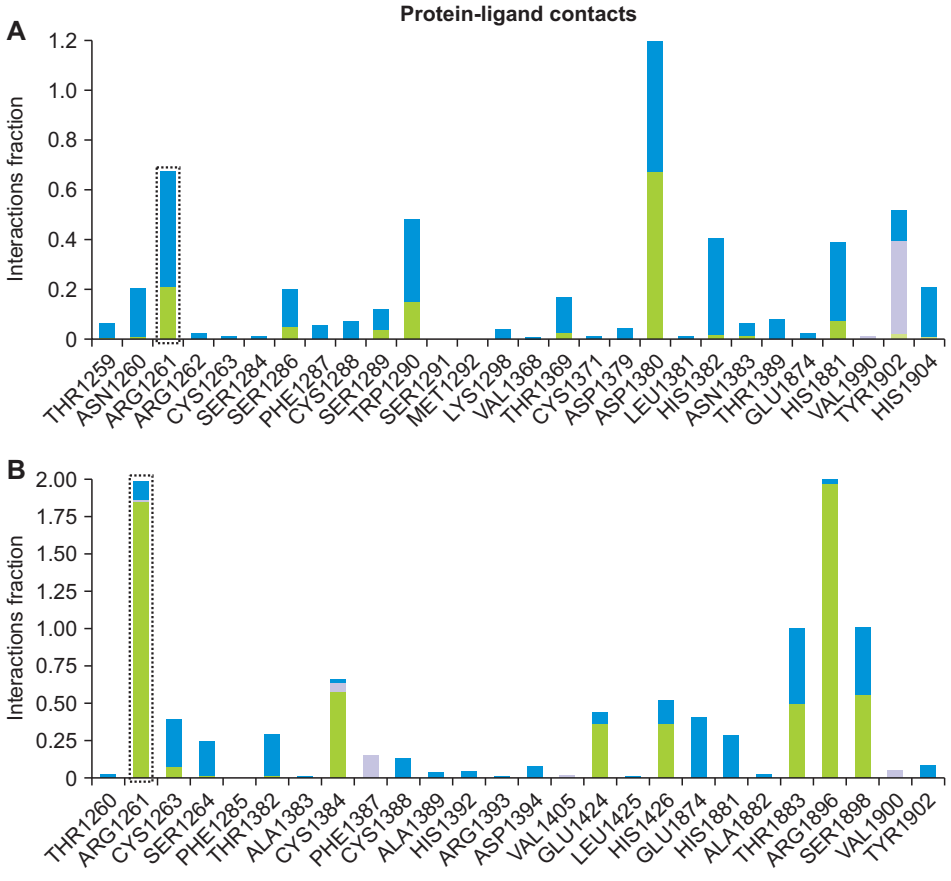

Figure 12. Protein-ligand contact map shows the inhibitory site binding by organic acids to TET2. MD simulations for 20 ns derived ligand-protein contact map of c-Raf kinase in complex with (A) β-KG-TET2 (A) and (B) Citrate-TET2 (B). TET2, Ten-Eleven Translocation-2; MD, molecular dynamic; β-KG, β-ketoglutarate.

epigenetic landscape and possibly induce genetic instability in cancer cells. Interestingly, SABFI contains both 2-hydroxyglutarate and its lactonized product, such as 2-hydroxyglutarate-γ-lactone. We also showed the binding of 2-hydroxyglutarate with TET2 as a competitive inhibitor compared to a natural substrate α-KG.

Molecular and structural studies suggest that crucial amino acid residues including ARG1261, HIS1382, HIS1416, HIS1881, ARG1896, and SER1898 are essential for the binding of α-KG as a substrate of TET2 for demethylase activity. Our data-based molecular docking and MD simulations indicated the binding amino acid residues such as ARG1261, HIS1382, HIS1416, HIS1881, ARG1896, and SER1898 in the case of SABFI-derived organic acids. Since then, SABFI induced proliferation arrest in treated oral cancer cells.

The implications of epigenetic regulation in OSCC are explored at molecular, cellular, and clinical levels. TET2 function is reduced and 5-hmC is lost among other epigenetic modifications and erasers [23-26]. It is important to note that the expression of TET2 in normal oral mucosal tissue is high [23-25]. There is a possibility that SABFI-derived organic acids are involved, which can inhibit TET2 function and cause a decrease in 5-hmC levels. Therefore, the present findings open up discussion on the interference of SABFI-derived organic acids in both normal oral mucosal cells and transformed OSCC cells by blocking the activity of TET2 and, in turn, the low level of 5-hmC.

A discussion on the relevance of TET2 expression to oral cancer is vital to understand the effects of SABFI-derived organic acids. Existing protein expression data on TET2 suggests a high level of TET1 in oral tissues [23-27]. Conversely, there is reduced expression of TET2 and loss of activity of TET2 in head and neck squamous cell carcinoma [25]. Aside from reduced expression, it is proposed that SABFI-derived organic acids can inhibit TET2 activity in oral mucosal tissues during initial exposures. Hence, TET2-mediated epigenetic alterations as one of the possible mechanisms behind BQ-mediated OSMF-OSCC.

The link between global DNA hypomethylation and oral cancer is scarcely discussed compared to lymphomas and other solid tumors. Multifactorial possibilities can induce hypomethylation of DNA and histone by losing the function of demethylases, including TET2, and potential inhibition by organic acids. In our observations, SABFI-derived organic acids such as 2-hydroxyglutarate, citrate, fumarate, malate, succinate, and β-KG are indicated to serve as potential competitive inhibitors of TET2. This may contribute to DNA hypomethylation during chronic exposure to SABFI by BQ users. After the initiation of OSMF-OSCC, the contribution of SABFI-derived organic acids such as 2-hydroxyglutarate, citrate, fumarate, malate, succinate, and β-KG during constant exposure of OSMF-OSCC cells may worsen the DNA methylation landscape that may lead to the generation of highly resistant and metastatic oral cancer cells.

TET2 induces global hypomethylation in cancer genomes but also synergizes with localized hypermethylation [46,47,50-58]. This process may explain why the epigenetic landscape in cancer cells during SABFI exposure is potentially altered due to TET2 inhibition. Such alterations of epigenetic marks in cancer cells may regulate the transcriptional gene regulation of DNA repair and cell cycle checkpoints. Hence, SABFI treatment of oral cancer cells leads to a proliferative arrest.

The role of TET2 is associated with alleviating oxidative stress in cancer cells. Hence, inhibition of TET2 could be linked with enhanced DNA damage and oxidative stress [50-58]. Such cellular conditions may push oral cancer cells toward proliferative arrests with high genomic instability. The findings of this paper fall in similar contexts with the SABFI-derived organic acids as an inhibitor of TET2 and cell-based data suggesting the arrest of proliferation in the case of oral cancer cells.

In recent studies, TET2 and histone demethylases are suggested as key epigenetic erasers that link epigenetic control with the maintenance of genome stability in cancer cells [55-58]. Conversely, loss of function and inhibition of TET2 and histone demethylases are proposed as a potential pathway that induces genomic instability by compromising DNA damage response to double-strand breaks that may be endogenous or due to environmental agents [53-58].

Data suggest that the accumulation of organic acids such as fumarate and succinate may induce defects in homologous-recombination DNA repair and genomic instability in cancer cells [53-58]. The molecular basis for fumarate and succinate's inhibitory effects on histone demethylases KDM4A and KDM4B is proposed. OSMF-OSCC is one kind of model that faces the exposure of SABFI-derived organic acids such as fumarate, malate, and succinate and, therefore, potential accumulation of genomic instability in exposed cells. Our data support similar observations that the accumulation of SABFI-derived organic acids is an inhibitor of DNA demethylases and stalls the proliferation of exposed cells, potentially due to genomic instability. In line with the potential role of organic acids in genomic instability in chronically exposed cells, such as in the case of OSMF, some persistent leader cells with a vicious cycle of exposure by SABFI-derived organic acids may show high genomic instability and altered methylation status. In turn, SABFI-derived organic acids may lead to the generation of persistent leader cells, and a similar proposition is discussed in potential tissue environments such as OSMF that lead to a high chance of malignant transformation in OSMF-OSCC.

Emerging views link DNA methylation status and cancer immunity in the context of solid tumors [19-22]. However, cancer immunity concerning OSMF-OSCC is not highlighted. An interesting paper emphasizes the role of TET2 in promoting programmed cell death ligand 1 (PD-L1) expression and c lymphocyte infiltration and cancer immunity [19]. Our findings suggested the relevance of SABFI-derived organic

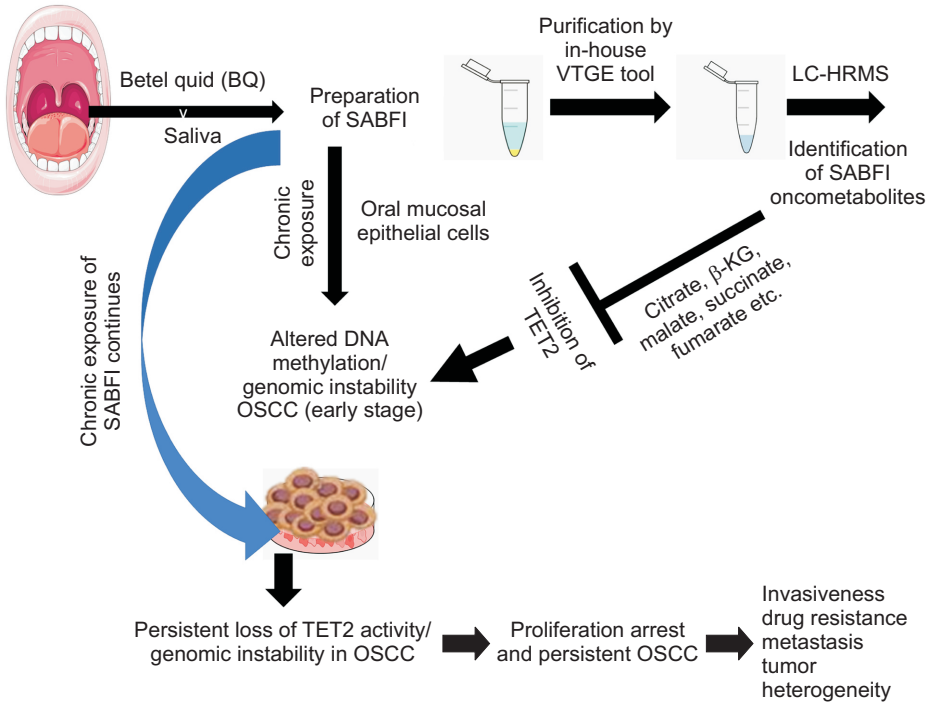

Figure 13. A flow model on the role of SABFI-derived organic acids as a potential inhibitor of TET2 DNA demethylase. Due to TET2 inhibition, SABFI-derived organic acids are proposed as contributors to genomic instability and proliferation arrests of chronically exposed oral mucosal epithelial cells and in the later stage oral cancer cells that may lead to persistent oral cancer cells. SABFI, saliva-amalgamated betel quid filtrate; TET2, Ten-Eleven Translocation-2; VTGE, vertical tube gel electrophoresis; LC-HRMS, liquid chromatography-high resolution mass spectrometry; β-KG, β-ketoglutarate; OSCC, oral squamous cell carcinoma.

acids such as β-KG, citric acid, 2-hydroxyglutarate, fumarate, malate, succinate, and β-KG as potential inhibitors of TET2. Further, this encouraged us to link the role of SABFI as a modulator of cancer immunity. Hence, the loss of activity of TET2 due to SABFI-derived organic acids may create a compromised cancer immunity by loss of PD-L1 expression in OSMF-OSCC. The relevance of SABFI organic acids needs emphasis for their immunomodulatory role in the early stage of OSMF-OSCC during continuous exposure to these organic acids. Besides the role of SABFI-derived organic acids as inhibitors of DNA and histone demethylases, they are known to promote tumorigenesis by inducing DNA breaks, oxidative stress, and intracellular signaling molecules of pro-growth signaling cascades [46,47]. Our observations compel preclinical and clinical scientists to revisit the association between BQ and oral cancer risk. A decades-old paper suggested that only *N*-nitrosoguvacoline among several classes of nitrosamines related to BQ could be detected in the saliva of users [5-7]. Interestingly, data suggested that the abundance of *N*-nitrosoguvacoline and other nitrosamines in the saliva of Indian BQ was much less compared to the saliva of users of green betel nut alone. Our methodology to extract and identify components of BQ-derived organic acids is closer to that published paper [5]. The existing paper employed the right approach to estimate BQ-derived genotoxic and organic acids that can leach out in the saliva microenvironment [5]. Hence, the risk of oral cancer and genotoxicity due to BQ-derived nitrosamines in the saliva of BQ users needs re-evaluation with better simulated experimental conditions. So a pertinent question is whether it is formidable to know the role of BQ-derived organic acids other than nitrosamines that can unleash metabolic-epigenetic alterations that, in the long term of exposure, may potentiate the initiation and progression of oral cancer.

A summarized illustration is presented to link the SABFI-derived organic acids and oral cancer (Fig. 13).

ACKNOWLEDGMENTS

The authors acknowledge research facilities extended by Bioinformatics Research Lab, DST-FIST sponsored Research facility and Central Research Facility, Dr. D. Y. Patil Vidyapeeth, Pune, MH, India.

FUNDING

The authors acknowledge CSIR-UGC, Government of India, for the Ph.D. Research Fellowship awarded to Ms. Devyani Bhatkar. We acknowledge an intramural seed grant from Dr. D. Y. Patil Vidyaoeeth, Pune, India, awarded to Prof. Dr. Nilesh Kumar Sharma (Ref. DPU/01/12/2020).

CONFLICTS OF INTEREST

No potential conflicts of interest were disclosed.

SUPPLEMENTARY MATERIALS

Supplementary materials can be found via https://doi.org/10.15430/JCP.2023.28.3.115.

ORCID

Devyani Bhatkar, https://orcid.org/0009-0006-5298-9465
Nistha Ananda, https://orcid.org/0000-0001-5430-5334
Kiran Bharat Lokhande, https://orcid.org/0000-0001-6945-8288
Kratika Khunteta, https://orcid.org/0000-0002-7912-8431
Priyadarshini Jain, https://orcid.org/0009-0002-1115-0437
Ameya Hebale, https://orcid.org/0000-0002-7265-4404
Sachin C. Sarode, https://orcid.org/0000-0003-1856-0957
Nilesh Kumar Sharma, https://orcid.org/0000-0002-8774-3020

REFERENCES

1. Sung H, Ferlay J, Siegel RL, Laversanne M, Soerjomataram I, Jemal A, et al. Global Cancer Statistics 2020: GLOBOCAN estimates of incidence and mortality worldwide for 36 cancers in 185 countries. CA Cancer J Clin 2021;71:209-49.
2. Hanahan D, Weinberg RA. Hallmarks of cancer: the next generation. Cell 2011;144:646-74.
3. Ward PS, Thompson CB. Metabolic reprogramming: a cancer hallmark even warburg did not anticipate. Cancer Cell 2012;21: 297-308.
4. Pavlova NN, Thompson CB. The emerging hallmarks of cancer metabolism. Cell Metab 2016;23:27-47.
5. Stich HF, Rosin MP, Brunnemann KD. Oral lesions, genotoxicity and nitrosamines in betel quid chewers with no obvious increase in oral cancer risk. Cancer Lett 1986;31:15-25.
6. Wenke G, Rivenson A, Brunnemann KD, Hoffmann D, Bhide SV. A study of betel quid carcinogenesis. II. Formation of N-nitrosamines during betel quid chewing. IARC Sci Publ 1984; (57):859-66.
7. Nair U, Bartsch H, Nair J. Alert for an epidemic of oral cancer due to use of the betel quid substitutes gutkha and pan masala: a review of agents and causative mechanisms. Mutagenesis 2004;19:251-62.
8. Madathil SA, Rousseau MC, Wynant W, Schlecht NF, Netuveli G, Franco EL, et al. Nonlinear association between betel quid chewing and oral cancer: implications for prevention. Oral Oncol 2016;60:25-31.
9. Lee HH, Chen LY, Wang HL, Chen BH. Quantification of salivary arecoline, arecaidine and N-methylnipecotic acid levels in volunteers by liquid chromatography-tandem mass spectrometry. J Anal Toxicol 2015;39:714-9.
10. Sarode SC, Chaudhary M, Gadbail A, Tekade S, Patil S, Sarode GS. Dysplastic features relevant to malignant transformation in atrophic epithelium of oral submucous fibrosis: a preliminary study. J Oral Pathol Med 2018;47:410-6.
11. Chamoli A, Gosavi AS, Shirwadkar UP, Wangdale KV, Behera SK, Kurrey NK, et al. Overview of oral cavity squamous cell carcinoma: risk factors, mechanisms, and diagnostics. Oral Oncol 2021;121:105451.
12. Pasupuleti RR, Lee CH, Osborne PG, Wu MT, Ponnusamy VK. Rapid green analytical methodology for simultaneous biomonitoring of five toxic areca nut alkaloids using UHPLC-MS/MS for predicting health hazardous risks. J Hazard Mater 2022;422:126923.
13. Tsai CL, Tainer JA. Probing DNA by 2-OG-dependent dioxygenase. Cell 2013;155:1448-50.
14. Yang M, Soga T, Pollard PJ. Oncometabolites: linking altered metabolism with cancer. J Clin Invest 2013;123:3652-8.
15. Cheishvili D, Boureau L, Szyf M. DNA demethylation and invasive cancer: implications for therapeutics. Br J Pharmacol 2015;172:2705-15.
16. Rasmussen KD, Helin K. Role of TET enzymes in DNA methylation, development, and cancer. Genes Dev 2016;30:733-50.
17. Zhang YW, Wang Z, Xie W, Cai Y, Xia L, Easwaran H, et al. Acetylation enhances TET2 function in protecting against abnormal DNA methylation during oxidative stress. Mol Cell 2017;65:323-35.
18. López-Moyado IF, Tsagaratou A, Yuita H, Seo H, Delatte B, Heinz S, et al. Paradoxical association of TET loss of function with genome-wide DNA hypomethylation. Proc Natl Acad Sci USA 2019;116:16933-42.
19. Xu YP, Lv L, Liu Y, Smith MD, Li WC, Tan XM, et al. Tumor suppressor TET2 promotes cancer immunity and immunotherapy efficacy. J Clin Invest 2019;129:4316-31.
20. Feng Y, Li X, Cassady K, Zou Z, Zhang X. TET2 function in hematopoietic malignancies, immune regulation, and DNA repair. Front Oncol 2019;9:210.
21. Bray JK, Dawlaty MM, Verma A, Maitra A. Roles and regulations of TET enzymes in solid tumors. Trends Cancer 2021;7:635-46.
22. Shukla V, Samaniego-Castruita D, Dong Z, González-Avalos E, Yan Q, Sarma K, et al. TET deficiency perturbs mature B cell homeostasis and promotes oncogenesis associated with accumulation of G-quadruplex and R-loop structures. Nat Immunol 2022;23:99-108.
23. Jäwert F, Hasséus B, Kjeller G, Magnusson B, Sand L, Larsson L. Loss of 5-hydroxymethylcytosine and TET2 in oral squamous cell carcinoma. Anticancer Res 2013;33:4325-8.
24. Cuevas-Nunez MC, Gomes CBF, Woo SB, Ramsey MR, Chen XL, Xu S, et al. Biological significance of 5-hydroxymethylcytosine in oral epithelial dysplasia and oral squamous cell carcinoma. Oral Surg Oral Med Oral Pathol Oral Radiol 2018;125:59-73.e2.
25. Huang R, Wang Y, Ge H, Wang D, Wang Y, Zhang W, et al. Restoration of TET2 deficiency inhibits tumor growth in head neck squamous cell carcinoma. Ann Transl Med 2020;8:329.
26. Zhang X, Yang J, Shi D, Cao Z. TET2 suppresses nasopharyngeal carcinoma progression by inhibiting glycolysis metabolism. Cancer Cell Int 2020;20:363.
27. Uhlén M, Fagerberg L, Hallström BM, Lindskog C, Oksvold P, Mardinoglu A, et al. Proteomics. Tissue-based map of the human proteome. Science 2015;347:1260419.
28. Xu W, Yang H, Liu Y, Yang Y, Wang P, Kim SH, et al. Oncometabolite 2-hydroxyglutarate is a competitive inhibitor of α-ketoglutarate-dependent dioxygenases. Cancer Cell 2011; 19:17-30.
29. Chowdhury R, Yeoh KK, Tian YM, Hillringhaus L, Bagg EA, Rose NR, et al. The oncometabolite 2-hydroxyglutarate inhibits histone

lysine demethylases. EMBO Rep 2011;12:463-9.
30. Xiao M, Yang H, Xu W, Ma S, Lin H, Zhu H, et al. Inhibition of α-KG-dependent histone and DNA demethylases by fumarate and succinate that are accumulated in mutations of FH and SDH tumor suppressors. Genes Dev 2012;26:1326-38. Erratum in: Genes Dev 2015;29:887.
31. Berger RS, Wachsmuth CJ, Waldhier MC, Renner-Sattler K, Thomas S, Chaturvedi A, et al. Lactonization of the oncometabolite D-2-hydroxyglutarate produces a novel endogenous metabolite. Cancers (Basel) 2021;13:1756.
32. Sarode SC, Sharma NK, Sarode G, Bhatkar D. Do osmotic pressure and hygroscopicity of areca nut related products drive extracellular fluid loss and condensation of collagen bundles in oral submucous fibrosis? Med Hypotheses 2022;163:110836.
33. Kumar A, Bhatkar D, Jahagirdar D, Sharma NK. Non-homologous end joining inhibitor SCR-7 to exacerbate low-dose doxorubicin cytotoxicity in HeLa cells. J Cancer Prev 2017;22:47-54.
34. Kumar A, Patel S, Bhatkar D, Sarode SC, Sharma NK. A novel method to detect intracellular metabolite alterations in MCF-7 cells by doxorubicin induced cell death. Metabolomics 2021;17:3.
35. Morris GM, Goodsell DS, Halliday RS, Huey R, Hart WE, Belew RK, et al. Automated docking using a Lamarckian genetic algorithm and an empirical binding free energy function. J Comput Chem 1998;19:1639-62.
36. Trott O, Olson AJ. AutoDock Vina: improving the speed and accuracy of docking with a new scoring function, efficient optimization, and multithreading. J Comput Chem 2010;31:455-61.
37. Accelrys Software Inc. The manual of Discovery Studio Visualizer v3.0. San Diego: Accelrys Software Inc., 2010.
38. Berry WL, Janknecht R. KDM4/JMJD2 histone demethylases: epigenetic regulators in cancer cells. Cancer Res 2013;73:2936-42.
39. Schrödinger. The manual of Release 2019-4: Desmond Molecular Dynamics System, D. E. Shaw Research. New York: Schrödinger, 2019.
40. Chang MC, Ho YS, Lee PH, Chan CP, Lee JJ, Hahn LJ, et al. Areca nut extract and arecoline induced the cell cycle arrest but not apoptosis of cultured oral KB epithelial cells: association of glutathione, reactive oxygen species and mitochondrial membrane potential. Carcinogenesis 2001;22:1527-35.
41. Khazaei S, Esa NM, Ramachandran V, Hamid RA, Pandurangan AK, Etemad A, et al. In vitro antiproliferative and apoptosis inducing effect of *Allium atroviolaceum* bulb extract on breast, cervical, and liver cancer cells. Front Pharmacol 2017;8:5.
42. Ohshima M, Sugahara K, Kasahara K, Katakura A. Metabolomic analysis of the saliva of Japanese patients with oral squamous cell carcinoma. Oncol Rep 2017;37:2727-34.
43. Pushalkar S, Ji X, Li Y, Estilo C, Yegnanarayana R, Singh B, et al. Comparison of oral microbiota in tumor and non-tumor tissues of patients with oral squamous cell carcinoma. BMC Microbiol 2012;12:144.
44. Hur H, Paik MJ, Xuan Y, Nguyen DT, Ham IH, Yun J, et al. Quantitative measurement of organic acids in tissues from gastric cancer patients indicates increased glucose metabolism in gastric cancer. PLoS One 2014;9:e98581.
45. Shinohara Y, Washio J, Kobayashi Y, Abiko Y, Sasaki K, Takahashi N. Hypoxically cultured cells of oral squamous cell carcinoma increased their glucose metabolic activity under normoxic conditions. PLoS One 2021;16:e0254966.
46. Toyokuni S, Sagripanti JL. Induction of oxidative single- and double-strand breaks in DNA by ferric citrate. Free Radic Biol Med 1993;15:117-23.
47. Tretter L, Patocs A, Chinopoulos C. Succinate, an intermediate in metabolism, signal transduction, ROS, hypoxia, and tumorigenesis. Biochim Biophys Acta 2016;1857:1086-101.
48. Fahrner JA, Baylin SB. Heterochromatin: stable and unstable invasions at home and abroad. Genes Dev 2003;17:1805-12.
49. Chang MC, Chan CP, Wang WT, Chang BE, Lee JJ, Tseng SK, et al. Toxicity of areca nut ingredients: activation of CHK1/CHK2, induction of cell cycle arrest, and regulation of MMP-9 and TIMPs production in SAS epithelial cells. Head Neck 2013;35:1295-302.
50. Mosammaparast N, Kim H, Laurent B, Zhao Y, Lim HJ, Majid MC, et al. The histone demethylase LSD1/KDM1A promotes the DNA damage response. J Cell Biol 2013;203:457-70.
51. Jiang Y, Qian X, Shen J, Wang Y, Li X, Liu R, et al. Local generation of fumarate promotes DNA repair through inhibition of histone H3 demethylation. Nat Cell Biol 2015;17:1158-68. Erratum in: Nat Cell Biol 2018;20:1226.
52. Wang P, Wu J, Ma S, Zhang L, Yao J, Hoadley KA, et al. Oncometabolite D-2-hydroxyglutarate inhibits ALKBH DNA repair enzymes and sensitizes IDH mutant cells to alkylating agents. Cell Rep 2015;13:2353-61.
53. Coulter JB, Lopez-Bertoni H, Kuhns KJ, Lee RS, Laterra J, Bressler JP. TET1 deficiency attenuates the DNA damage response and promotes resistance to DNA damaging agents. Epigenetics 2017;12:854-64.
54. Wentzel JF, Lewies A, Bronkhorst AJ, van Dyk E, du Plessis LH, Pretorius PJ. Exposure to high levels of fumarate and succinate leads to apoptotic cytotoxicity and altered global DNA methylation profiles in vitro. Biochimie 2017;135:28-34.
55. Chen LL, Lin HP, Zhou WJ, He CX, Zhang ZY, Cheng ZL, et al. SNIP1 recruits TET2 to regulate c-MYC target genes and cellular DNA damage response. Cell Rep 2018;25:1485-500.e4.
56. Janssen A, Colmenares SU, Lee T, Karpen GH. Timely double-strand break repair and pathway choice in pericentromeric heterochromatin depend on the histone demethylase dKDM4A. Genes Dev 2019;33:103-15.
57. Maifrede S, Le BV, Nieborowska-Skorska M, Golovine K, Sullivan-Reed K, Dunuwille WMB, et al. *TET2* and *DNMT3A* mutations exert divergent effects on DNA repair and sensitivity of leukemia cells to PARP inhibitors. Cancer Res 2021;81:5089-101.
58. Mahfoudhi E, Talhaoui I, Cabagnols X, Della Valle V, Secardin L, Rameau P, et al. TET2-mediated 5-hydroxymethylcytosine induces genetic instability and mutagenesis. DNA Repair (Amst) 2016;43:78-88.